

Supporting Information for

Radical qubits photo-generated in acene-based metal-organic frameworks

Kana Orihashi,^{#a} Akio Yamauchi,^{#a} Miku Inoue,^a Bhavesh Parmar,^a Saiya Fujiwara,^b Nobuo Kimizuka,^a Mizue Asada,^c Toshikazu Nakamura,^c and Nobuhiro Yanai^{*a,d}

^aDepartment of Applied Chemistry, Graduate School of Engineering, Center for Molecular Systems (CMS), Kyushu University, 744 Moto-oka, Nishi-ku, Fukuoka 819-0395, Japan.

^bRIKEN Center for Emergent Matter Science, Riken, Wako, Saitama 351-0198, Japan.

^cInstitute for Molecular Science, Nishigonaka 38, Myodaiji, Okazaki 444-8585, Japan.

^dFOREST, CREST, JST, Honcho 4-1-8, Kawaguchi, Saitama 332-0012, Japan.

Materials

All reagents were used as purchased unless otherwise noted. Naphthalene-2,3-diol, benzene-1,2-diamine, $K_2Cr_2O_7$, sodium sulfate, bromine, and cesium carbonate were purchased from FUJIFILM Wako pure chemical. Acetic acid, hydrochloric acid, and sodium hydroxide were purchased from KISHIDA. 4-(4,4,5,5-tetramethyl-1,3,2-dioxaborolan-2-yl)pyridine, 4-(methoxycarbonyl)phenylboronic acid, tetrakis(triphenylphosphine)-palladium(0), 4,4'-biphenyldicarboxylic acid, and terephthalic acid were purchased from TCI. 1,2,4,5-Tetrakis(4-carboxyphenyl)benzene was purchased from Sigma Aldrich.

General characterizations

1H -NMR spectra were measured on a JEOL JNM-ECZ-400 spectrometer using TMS as the internal standard. Elemental analysis was carried out by using a Yanaco CHN Corder MT-5 at the Elemental Analysis Center, Kyushu University. Single crystal X-ray data were collected on a CCD diffractometer (Rigaku XtaLAB Synergy-R/DW) with graphite-monochromate Mo $K\alpha$ radiation ($\lambda_{ex} = 0.7170 \text{ \AA}$). Powder X-ray diffraction (PXRD) patterns were measured on a Bruker D2 Phaser (Cu- $K\alpha$, 30 kV 10 mA). Thermogravimetric analysis curves were obtained on a Rigaku Thermo Plus EVO2 under N_2 . UV-Vis absorption spectra were recorded on a JASCO V-670 spectrometer. Diffuse reflection methods were employed for solid samples.

ESR spectroscopy

Steady state continuous wave electron spin resonance (CW-ESR) spectra were measured on a Bruker EMX 8/2.7 at X-band ($\sim 9.6 \text{ GHz}$) using a glass capillary (FPT-220, FUJISTON, diameter 2.2 mm, inner diameter 1.4 mm) placed into a 4 mm quartz ESR tubes. Pulsed laser irradiation with wavelength, frequency, power, and duration of 532 nm, 10 Hz, 7.6 mJ, and 20 min, respectively, were applied prior to the ESR measurements using a pulsed Nd:YAG laser (Continuum, Surelite I).

Pulsed ESR measurements were performed on a Bruker E680 operated at X-band ($\sim 9.6 \text{ GHz}$) using a glass capillary (FPT-220, FUJISTON, diameter 2.2 mm, inner diameter 1.4 mm) placed into a 4 mm quartz ESR tubes. A Bruker standard dielectric resonator was used as a microwave resonator (ER4118X-MD5W) using TE011 mode. The samples were photo-excited at a wavelength of 532 nm, excitation light intensity of 2-3 mJ/pulse, repetition rate of 30 Hz, and pulse length of 5-12 ns using a Spectra-Physics Quanta-Ray Nd:YAG laser for 5 min prior to the measurements. The microwave intensities were $\sim 0.06 \text{ mW}$ for time-resolved measurements unless otherwise noted. For pulsed ESR measurements, $\sim 2 \text{ \mu W}$ of microwave irradiation was amplified to a fix $\pi/2$ pulse of 16 ns. Inversion recovery measurements were conducted using a three-pulse spin echo sequence. The first π pulse was irradiated, with an interval τ before the second $\pi/2$ pulse being varied. The third pulse irradiated after 0.2 μs of interval, and then the echo signal followed after 0.2 μs of interval was observed. T_1 was obtained by single exponential fitting of recovery curves. The echo decay measurements were conducted using a two-pulse spin echo sequence. The pulse interval τ between the first $\pi/2$ pulse and the second $\pi/2$ pulse was varied, and then the echo signal followed after 0.2 μs of interval was observed. T_2 was obtained by single exponential fitting of decay curves. $\pi/2$ pulse and π pulse were fixed as 16 ns and 24 ns, respectively.

For ESR measurements, the MOF crystals dried under vacuum at room temperature was dispersed in paraffin to prevent damage from laser-irradiation. The dispersed samples were packed into a glass capillary (FPT-220, FUJISTON, diameter 2.2 mm, inner diameter 1.4 mm), deaerated using a vacuum line to remove oxygen in the sample liquid, and then flame-sealed.

Synthesis of DPyDAT

DPyDAT was synthesized according to the reported procedure.¹

Synthesis of DAT-MOF-1

DPyDAT (19.2 mg, 0.049 mmol), 4,4'-biphenyldicarboxylic acid (**BPDC**) (24.2 mg, 0.10 mmol), and $\text{Zn}(\text{NO}_3)_2 \cdot 6\text{H}_2\text{O}$ (29.7 mg, 0.01 mmol) were dissolved in 6.0 ml of DMF and heated at 100 °C for 24 hours. 46.3 mg of DAT-MOF-1 as orange plate-like crystals were obtained (yield: 46.2%).

Elemental analysis for the MOF powder, calculated for $[\text{Zn}_2(\text{BPDC})_2(\text{DPyDAT})] \cdot 1.5\text{H}_2\text{O}$ ($\text{C}_{54}\text{H}_{35}\text{N}_4\text{O}_{9.5}\text{Zn}_2$) H:3.45, C:63.42, N:5.48; found H:3.22, C:63.46, N:5.65.

Synthesis of DAT-MOF-2

DPyDAT (12.0 mg, 0.03 mmol), 1,2,4,5-Tetrakis(4-carboxyphenyl)benzene (**TCPB**) (17.49 mg, 0.03 mmol), and $\text{Zn}(\text{NO}_3)_2 \cdot 6\text{H}_2\text{O}$ (17.85 mg, 0.06 mmol) were dissolved in 10 ml of DMF and heated at 100 °C for 24 hours. 51.2 mg of DAT-MOF-2 as red needlelike crystals were obtained (yield: 65.0 %).

Elemental analysis for the MOF powder, calculated for $[\text{Zn}_2(\text{TCPB})(\text{DPyDAT})] \cdot 3.2\text{DMF} \cdot 0.5\text{H}_2\text{O}$ ($\text{C}_{69.6}\text{H}_{57.4}\text{N}_{7.2}\text{O}_{11.7}\text{Zn}_2$) H:4.40, C:63.69, N:7.68; found H:4.40, C:63.78, N:7.48.

Synthesis of DAT-MOF-3

DPyDAT (12.0 mg, 0.03 mmol), terephthalic acid (**TA**) (11.0 mg, 0.07 mmol), and $\text{Zn}(\text{NO}_3)_2 \cdot 6\text{H}_2\text{O}$ (15.0 mg, 0.05 mmol) were dissolved in 10 ml of DMF and heated at 100 °C for 24 hours. 49.3 mg of DAT-MOF-3 as red crystals were obtained (yield: 69.4%).

Elemental analysis for the MOF powder, calculated for $[\text{Zn}_3(\text{TA})_3(\text{DPyDAT})] \cdot 1.5\text{DMF}$ ($\text{C}_{54.5}\text{H}_{38.5}\text{N}_{5.5}\text{O}_{13.5}\text{Zn}_3$) H:3.28, C:55.35, N:6.51; found H:3.37, C:55.48, N:6.67.

Detail of SCXRD and analyzed structure (DAT-MOF-2)

CCDC 2309918 contains the supplementary crystallographic data for this paper. These data can be obtained free of charge from The Cambridge Crystallographic Data Centre via www.ccdc.cam.ac.uk/structures.

Table S1. Summary of crystallographic data of DAT-MOF-2

Compound	DAT-MOF-2
formula	$C_{7.625}H_4N_{0.25}OZn_{0.25}$
formula weight	131.45
crystal color, habit	Orange, block
crystal system	orthorhombic
space group	Pmmm
a (Å)	11.0072
b (Å)	15.9706
c (Å)	18.2207
α (deg)	90
β (deg)	90
γ (deg)	90
V (Å ³)	3203.0
Z, Z'	$Z: 8 Z': 1$
ρ_{calcd} (g/cm ³)	0.545
$F(000)$	536
μ (mm ⁻¹)	0.651
T (K)	100
goodness-of-fit on F^2	1.096
R_{int}	0.0457
Final $R1$	0.0847
w $R2$	0.2463

Detail of SCXRD and analyzed structure (DAT-MOF-3)

CCDC 2309924 contains the supplementary crystallographic data for this paper. These data can be obtained free of charge from The Cambridge Crystallographic Data Centre via www.ccdc.cam.ac.uk/structures.

The SQUEEZE routine in PLATON2 was applied to remove the contributions of electron density from disordered guest DMF solvent molecules since its severe disorder hindered satisfactory development of the model.

Table S2. Summary of crystallographic data of DAT-MOF

Compound	DAT-MOF-3
formula	C ₁₀₀ H ₅₉ N ₈ O ₂₄ Zn ₆
formula weight	2148.77
crystal color, habit	Orange, plate
crystal system	triclinic
space group	P $\bar{1}$
<i>a</i> (Å)	18.5415
<i>b</i> (Å)	18.8522
<i>c</i> (Å)	23.5975
α (deg)	101.451
β (deg)	110.314
γ (deg)	90.019
<i>V</i> (Å ³)	7559.9
<i>Z</i>	2
ρ_{calcd} (g/cm ³)	0.944
<i>F</i> (000)	2174
μ (mm ⁻¹)	1.467
<i>T</i> (K)	100
goodness-of-fit on <i>F</i> ²	0.964
R _{int}	0.0599
Final R1	0.1110
wR2	0.3154

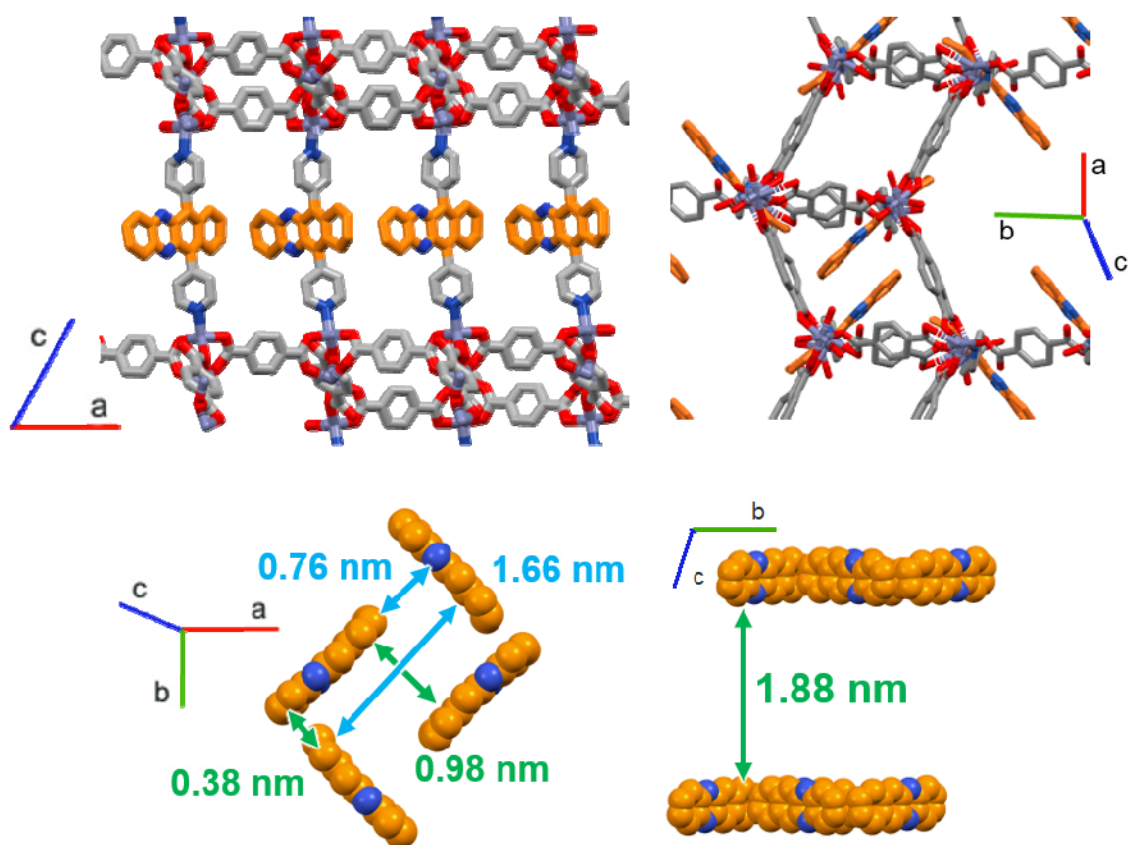


Figure S1. The single crystal structure of DAT-MOF-2 and arrangement of DAT in the MOF viewed along *a*, *b* and *c* axis.

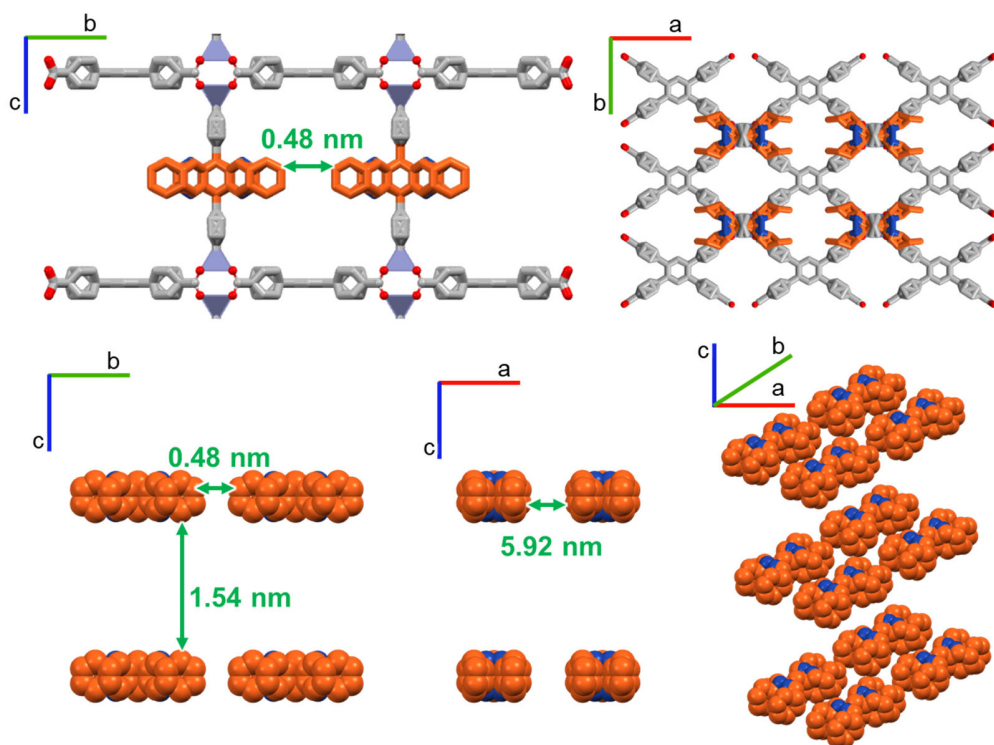


Figure S2. The single crystal structure of DAT-MOF-3 and arrangement of DAT in the MOF viewed along *a*, *b* and *c* axis.

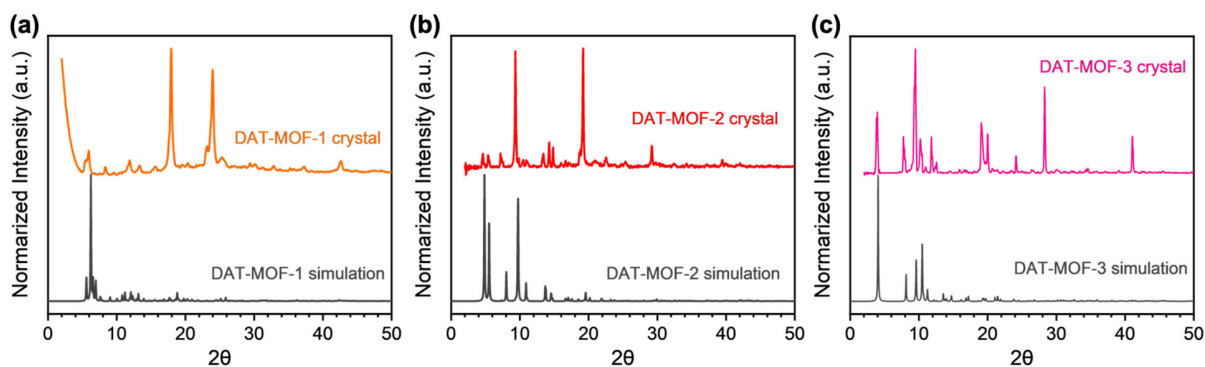


Figure S3. PXRD patterns of crystals of (a) DAT-MOF-1, (b) DAT-MOF-2, (c) DAT-MOF-3 obtained by solvothermal reaction (orange, pink, red lines, respectively). Simulated patterns by each crystal structure are also shown for comparison (gray lines).

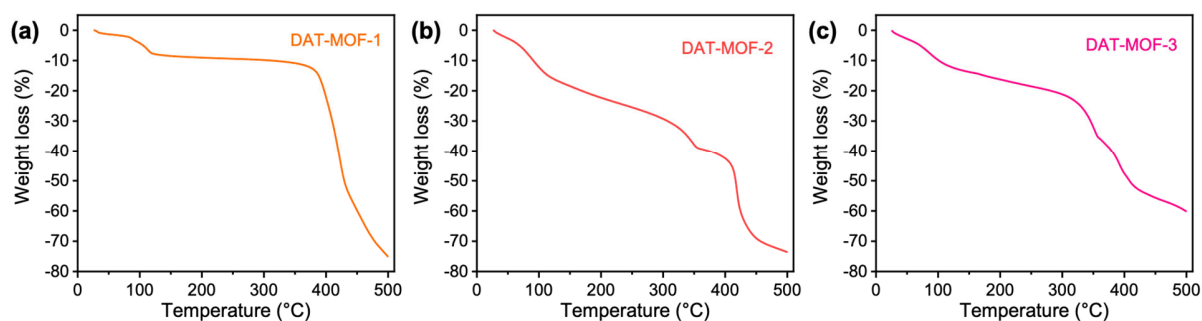


Figure S4. TGA curves of crystals of (a) DAT-MOF-1, (b) DAT-MOF-2, (c) DAT-MOF-3 with a heating rate of 5 °C/min under N₂.

References

- 1 K. Orihashi, A. Yamauchi, S. Fujiwara, M. Asada, T. Nakamura, J. K.-H. Hui, N. Kimizuka, K. Tateishi, T. Uesaka and N. Yanai, Spin-Polarized Radicals with Extremely Long Spin-Lattice Relaxation Time at Room Temperature in a Metal-Organic Framework, *ChemRxiv*, , DOI:10.26434/chemrxiv-2023-2mrsw.